Influence of crystalline defects on nitrogen implantation in copper for surface hardening

Ghenwa Zaher, Xavier Sauvage, Samuel Jouen

Scripta Materialia 231 (2023) 115440
https://doi.org/10.1016/j.scriptamat.2023.115440

Influence of crystalline defects on nitrogen implantation in copper for surface hardening

Ghenwa Zaher, Xavier Sauvage*, Samuel Jouen

Univ Rouen Normandie, INSA Rouen Normandie, CNRS, Groupe de Physique des Matériaux UMR 6634, 76000 Rouen, France

*Corresponding author : xavier.sauvage@univ-rouen.fr

Keywords: Copper; nitrogen; implantation; crystalline defects; hardness

Abstract

The design of electrical contacts that combine a high electrical conductivity and excellent wear resistance requires the optimization of surface processing. Surface hardening of copper was achieved by nitrogen implantation and the underlying mechanisms were investigated by electron microscopy. Pure copper and a CuSn alloy were implanted with nitrogen in the recrystallized state and after severe plastic deformation. The larger lattice parameter of CuSn does not promote the implantation of N but the large density of crystalline defects in the as-deformed material gives rise a much thicker implanted layer up to 120±20 nm. In all cases, the strong hardening results from a high density of nanoscaled Cu_3N particles (1.2±0.4 10^{23} m^{-3}). Deformation twins seem to promote both the diffusion and the nucleation of Cu_3N.

Graphical abstract

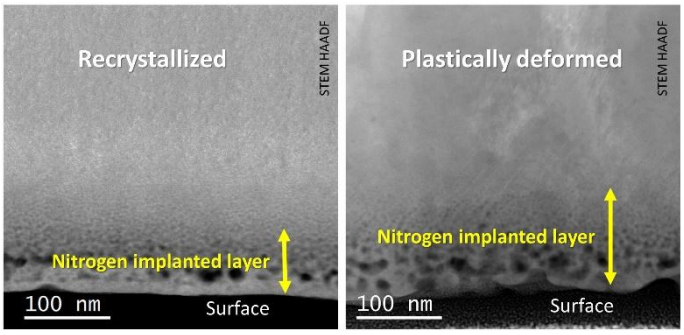

Copper and copper alloys play a major role in the electrical industry and in electronic devices. They are used for power lines, connectors and data transfer cables with various combination of properties depending on targeted applications. Pure copper exhibits a low electrical resistivity (ideal for power transfer) but its relatively low mechanical strength is a strong limitation for applications where tensile strength, fatigue or wear resistance is also required. Significant hardening can be obtained by strain hardening during cold working such as wire drawing, but the resulting high dislocation density can easily recover near room temperature. A small amount of alloying element in solid solution such as Sn help stabilizing the deformed structure and the thermal stability. The other alloying strategy is to use elements with a low solubility such as Cr and to carry out a precipitation treatment. In any case however, copper alloys exhibit a higher electrical resistivity as compared to pure copper due to the scattering of electrons by solutes (for example $\Delta\Omega \sim 3\ 10^{-8}$ Ωm/at.%Sn [1]). Besides, in some applications, like contactors, one of the major requirements is a high surface hardness to avoid excessive wear during service. Then, to preserve bulk electrical properties, only the surface has to be hardened. It has been shown that ion implantation of copper and copper alloys can be successfully applied using nitrogen, carbon or boron [2] and nitrogen implantation seems the most promising [3-8]. The equilibrium solubility of nitrogen in copper is extremely low and there is no Cu-N phase diagram reported in the literature [9]. Laffitte and co-authors were able to detect some N in solid solution in Cu only at temperatures higher than 900°C [10]. Three nitrides are reported for the Cu-N system (Cu_3N, CuN_3 and CuN_6 [9]) and it has been shown since a long time that Cu_3N could be easily obtained by chemical reactions between NH_3 and CuF_2 [11] or CuO [12]. Similar Cu_3N nitrides could also be obtained by ion implantation [4, 6-8] but this technique also leads sometimes to a different stoichiometry [3]. The Cu_3N phase exhibits a cubic crystallographic structure (Pm3m) with a lattice parameter of 0.3813nm [11], N atoms being inserted in octahedral sites of the fcc Cu [13]. This phase is not thermally stable and usually decomposes at temperatures above 100°C [14], it is also easily oxidized at room temperature in a humid atmosphere [15]. However, the nucleation of Cu_3N during implantation significantly increases the surface hardness and reduces the corrosion rate in acid media [7] or in contact of sodium chloride [16].

Crystalline defects, such as grain boundaries (GB) and dislocations, are known to play a significant role on diffusion by facilitating solute transport and also on precipitation by reducing the nucleation barrier of second phase particles. Therefore, they can significantly promote solute implantation as demonstrated by L. Ge and co-authors on a nitrided titanium alloy [17]. Besides, in case of coherent precipitation, the lattice misfit between the matrix and

the nucleated phase has a strong influence on the growth of particles [18]. Thus, the aim of this work was to evaluate the influence of both defects and misfit on nitrogen implantation. The lattice misfit was modified by alloying with Sn and defects were introduced using severe plastic deformation (SPD) prior to implantation.

Commercially pure copper (Cu-A1, 99.9% purity) and a CuSn8 (8wt.%Sn) alloy were processed by high pressure torsion (HPT). Discs (20mm diameter, thickness 1mm) were deformed at room temperature under a pressure of 6GPa up to 20 rotations at a speed of one rotation per minute. A previously published work shows that it leads to ultrafine grained (UFG) structures with a high fraction of grain boundaries in both materials [19]. To obtain a reference material with a low amount of defects, a recrystallization treatment was carried out at 600°C during 1h giving rise to a grain size of about 50μm.

Just before implantation, samples were mirror polished. Implantation was carried out with nitrogen ions using a Hardion+ implantor from Quertech Ingénierie [20]. Multiple charged ions (58% N^{+}, 32% N^{2+}, 9% N^{3+} and 1% N^{4+}) were accelerated with a voltage of 30kV providing a large implantation profile with a maximum near 50nm below the surface and extending up to 150nm (theoretical estimate calculated with the SRIM software). The estimated dose of implanted N is about 5 10^{7} ions/cm^{2}.

The resulting structures were characterized by transmission electron microscopy (TEM). Cross sectional samples were prepared by focused ion beam (FIB) with Ga ions in a N-vision40 (Zeiss®) instrument using a classical lift-out method. Microstructures were then observed in a JEOL® ARM-200F microscope operated at 200kV using a parallel beam for bright field imaging and selected area electron diffraction (SAED). Additional observations were carried out in Scanning-TEM (STEM) using High Angle Annular Dark Field Z-contrast imaging and dark field (collection angles 80-180 and 20-80 mrad respectively). Analytical data were also collected using Electron Energy Loss Spectroscopy (EELS) using a Gatan® Imaging Filter (GIF-quantum) with an energy spread of incident electrons of 0.7eV.

The surface hardness was evaluated by nano-indentation measurements using a TI 950 TriboIndenter Hysitron® with Berkovich indent and a penetration depth of 50nm (three times smaller than the theoretical implantation depth).

The nano-hardness of the recrystallized copper and of the copper processed by SPD with a UFG structure in the initial state and after nitrogen implantation are reported in Table 1. In the initial state, data do not exhibit any significant difference although the severely deformed

copper is expected to be much harder. This is due to the extremely small penetration depth that was used (50 nm). As detailed in the literature, it gives rise to typical high hardness [21, 22] without significant influence of GBs [23]. Nevertheless, after nitrogen implantation, a significant increase is observed in both materials indicating that near surface modifications occurred. The measured nano-hardness is however relatively similar for both materials (difference within the error bar), which indicates a negligible influence of GBs.

Table 1: Nano-hardness of the recrystallized Cu and UFG Cu (after SPD), before and after implantation with N.

Nano HV (GPa)	Recrystallized Cu	Cu UFG
initial	**1.8 ± 0.2**	**2.0 ± 0.2**
Implanted with N	**3.6 ± 0.5**	**3.3 ± 0.7**

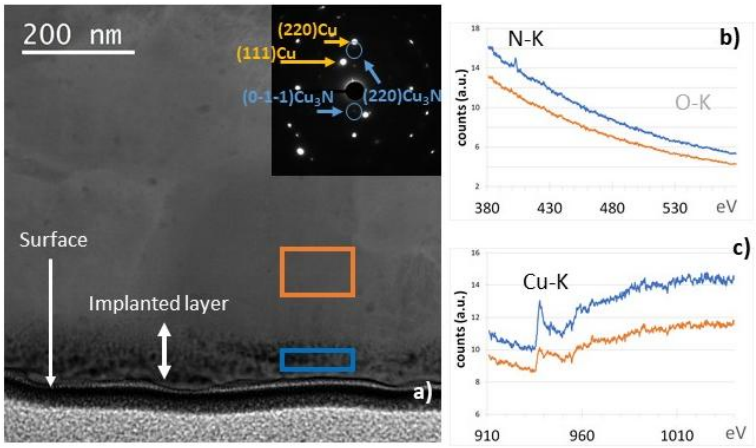

Figure1: Cross sectional view of the UFG copper implanted with nitrogen, a) STEM-HAADF image with the surface located at the bottom, inset SAED pattern recorded in the implanted zone, b) and c) EELS spectra recorded in the implanted layer (blue) and in the matrix (orange).

The cross section of the implanted UFG Cu is displayed in Fig. 1(a) where the HAADF image clearly exhibits a dark layer below the surface (located in the lower part of the image). This sub-surface layer contains a high density of darkly imaged nanoscaled particles. Since HAADF images provide a Z-contrast, these particles should contain elements lighter than Cu.

EELS measurements were carried out both in the subsurface area and in the bulk (blue and orange areas in Fig. 1(a) respectively). Spectra near the N-K and Cu-K edges are displayed in Fig. 1(b) and (c). They clearly show that some nitrogen (N-K edge at 402 eV) is detected in the subsurface region but not in the bulk. Thus the dark layer exhibited on the STEM-HAADF image in Fig. 1(a) corresponds to the implanted layer. In this layer, the O-K edge (532 eV) is not exhibited, indicating that surface oxidation did not occur during the process. Besides, the Cu-K edge is slightly different as compared to the bulk (Fig. 1 (c)), indicating that the local environment of Cu atoms might be slightly different. A careful examination of the selected area electron diffraction (SAED) pattern recorded in the subsurface region (Fig. 1(a) inset) shows that some spots could be attributed to the Cu_3N phase. And since the (220)Cu and the (220)Cu_3N spots are aligned, it indicates that some Cu_3N particles have grown coherently with the fcc Cu matrix. The UFG Cu exhibits a mean grain size of about 380nm with a relatively low dislocation density (see our previous work [19]) and no specific feature could be observed near GBs.

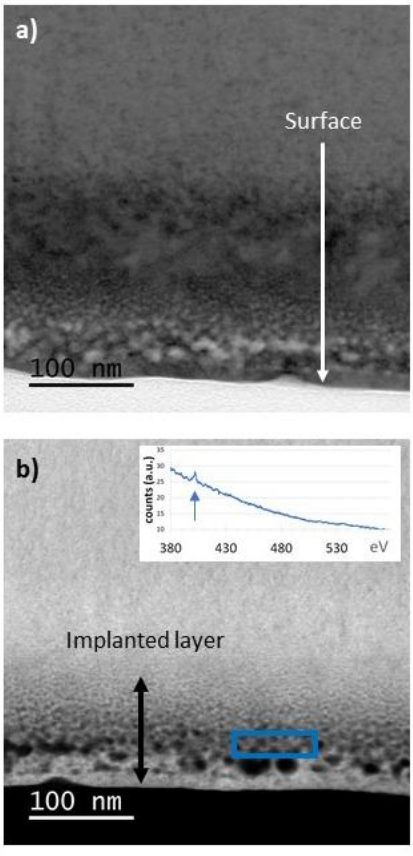

Figure2: Cross sectional view of the recrystallized CuSn8 alloy implanted with nitrogen with the surface located at the bottom, a) STEM-BF image, b) STEM-HAADF image with inset the EELS spectra recorded in the implanted layer showing a peak at the N-K edge

Very similar features were observed in the recrystallized CuSn8 alloy after nitrogen implantation (Fig. 2). Cu_3N particles are brightly imaged on the STEM-BF image (Fig. 2(a)) and darkly imaged by STEM-HAADF (Fig. 2(b)). In the subsurface region, the N-K edge (402 eV) clearly appear on the EELS spectrum (Fig. 2(b) inset) indicating that nitrogen was successfully implanted. This led to the growth in a subsurface layer of Cu_3N nanoscaled particles darkly imaged on the STEM HAADF image. The width of this subsurface implanted layer was measured in various locations, it ranges between 60 and 90nm which is somewhat smaller than the theoretical implantation depth (extending up to 150nm). As shown in table 2, this is very similar to the thickness measured in the implanted commercially pure Cu, indicating that the misfit reduction resulting from Sn alloying does not significantly modify the implantation depth. The misfit between fcc Cu and Cu_3N is about 5% (a~0.36 and ~0.38nm respectively [11]) while 8wt.% of Sn increases the lattice parameter of Cu of only about 2% [24]. Thus, this reduction of the misfit between the two phases might not be significant enough to promote the homogeneous nucleation and growth of the Cu_3N phase.

Table 2: Mean thickness of the implanted layers measured on STEM-HAADF images (the error bar is the distribution spread)

Cu UFG	**CuSn8 UFG**	**CuSn8 recrystallized**
73 ± 12 nm	**120 ± 20 nm**	**75 ± 15 nm**

After HPT, the mean grain size is much smaller in the CuSn8 alloy than in the commercially pure Cu (130 ± 60 nm against 380 ± 150 nm respectively) and a high density of crystalline defects, especially deformation twins, is introduced [19]. Although it cannot be excluded that the implantation process might locally affect this UFG structure, most of defects are retained and twins are arrowed on the STEM-DF image in Fig. 3(c). Similarly to Cu and recrystallized CuSn8 after implantation, a darkly imaged subsurface layer where nitrogen is detected by EELS is clearly exhibited on STEM-HAADF images (Fig. 3(a) and (d)). Nanoscaled Cu_3N particles have grown inside grains and careful examination of the structure did not reveal any specific contribution of GBs indicating that they do not act as specific nucleation site. As shown in Fig. 3(d), other crystalline defects, namely twin boundaries, seem however to play a critical role since Cu_3N particles are aligned in the same direction. The SAED pattern (Fig.

3(b)) recorded near a <111> fcc Cu zone axis shows that some particles are obviously coherent with the matrix while others do not exhibit any preferential orientation relationship (* label on the SAED pattern) and have most probably heterogeneously nucleated. The thickness of the implantation layer (dark subsurface layer on HAADF images) is 120±20nm in the UFG CuSn8 which is almost twice larger than in the recrystallized alloy (Table 2) and consistent with the theoretical implantation depth (extending up to 150nm). Thus, crystalline defects introduced by SPD and stabilized by Sn in solid solution [19] significantly affect the implantation of nitrogen in copper. Since twins do not affect the size of the octahedral sites in the fcc Cu lattice (location of N atoms forming the Cu_3N phase [13]), they should not promote the atomic transport of nitrogen, its local solubility or the nucleation of Cu_3N particles. However, these deformation twins were created by SPD and they typically contain many defects such as dislocation debris or vacancies [25] which probably promote the implantation of nitrogen.

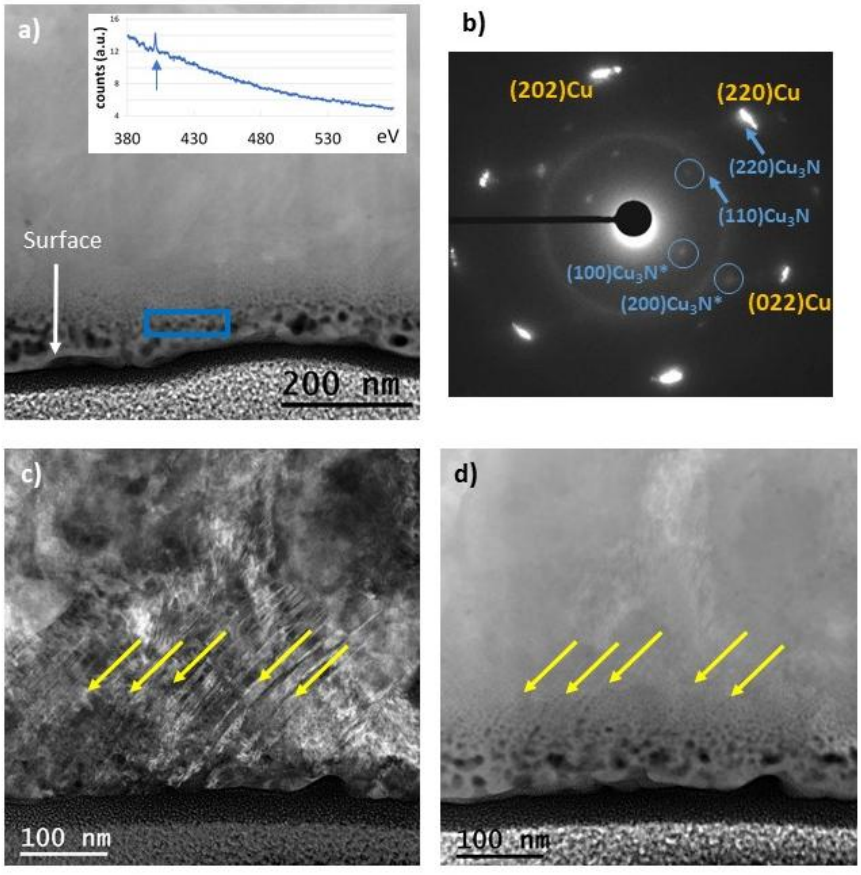

Figure3: Cross sectional view of the CuSn8 alloy processed by HPT implanted with nitrogen with the surface located at the bottom, a) STEM-HAADF image with inset the EELS spectra recorded in the implanted layer showing a peak at the N-K edge, b) SAED pattern recorded in the implanted layer near a <111>Cu zone axis showing some coherent and incoherent

*(*mark) Cu_3N particles, c) STEM BF image showing deformation twins (arrowed), d) STEM-HAADF image, same location like (c) and showing Cu_3N particles along twin boundaries*

The average number density of Cu_3N particles in the implanted layer was estimated in the UFG CuSn8 in a range of 0.8 to 1.6 10^{23} m^{-3}. Considering a mean diameter of particle of 10nm, it gives a volume fraction in a range of 4 to 8% corresponding to a mean concentration of implanted nitrogen of 1 to 2 at.% in the 120nm thick layer below the surface. This is about one order of magnitude smaller than the expected concentration estimated from the implantation dose (5 10^{17} ions cm^{-2}), indicating that a significant amount of nitrogen is desorbed from the surface during implantation.

In conclusion, this experimental work demonstrated that : i) nitrogen implantation is an effective process for surface hardening of copper and copper alloys; ii) the hardening results from the nucleation and growth of Cu_3N nanoparticles in a subsurface layer with a thickness of about 75±10 nm; iii) enlarging the lattice parameters of Cu by Sn alloying does not promote the implantation of nitrogen; iv) introducing a large density of defects by severe plastic deformation prior to implantation and especially twins gives rise to a much thicker implanted layer (120±20 nm). This is attributed to an enhanced nitrogen diffusion and a lower Cu_3N nucleation barrier. Thus, this work suggests that surface severe plastic deformation (SSPD) processes combined with implantation should be ideal to significantly enhance the wear resistance of electrical contacts made of copper or copper alloys.

Acknowledgements

Dr N. Enikeev and Dr I. Lomakin are gratefully acknowledged for material processing by HPT. F. Cuvilly is gratefully acknowledged for FIB sample preparation. This work was partially supported by the CNRS Federation IRMA - FR 3095.

References

[1] Kazunari Maki, Yuki Ito, Hirotaka Matsunaga, Hiroyuki Mori, Solid-solution copper alloys with high strength and high electrical conductivity, Scripta Materialia, Volume 68, Issue 10, 2013, Pages 777-780

[2] S. Saritas, R. P. M. Procter, V. Ashworth, and W. A. Grant, "The effect of ion implantation on the friction and wear behaviour of a phosphor bronze," *Wear*, vol. 82, no. 2, pp. 233– 255, Nov. 1982.

[3] P. D. Prabhawalker, D. C. Kothari, M. R. Nair, and P. M. Raole, "XPS studies at various temperatures of nitrogen implanted copper," *Nucl. Instrum. Methods Phys. Res. Sect. B Beam Interact. Mater. At.*, vol. 7–8, pp. 147–150, Mar. 1985.

[4] X. Zhou, H.-D. Li, and B. X. Liu, "Formation of noble-metal nitrides by nitrogen implantation," *Nucl. Instrum. Methods Phys. Res. Sect. B Beam Interact. Mater. At.*, vol. 39, no. 1, pp. 583–586, Mar. 1989.

[5] E. Ma, B. X. Liu, X. Chen, and H. D. Li, "Structural transformation induced by nitrogen implantation in thin metal films," *Thin Solid Films*, vol. 147, no. 1, pp. 49–55, Feb. 1987.

[6] L. J. Cristina, R. A. Vidal, and J. Ferrón, "Surface characterization of nitride structures on Cu(001) formed by implantation of N ions: An AES, XPS and LEIS study," *Surf. Sci.*, vol. 602, no. 21, pp. 3454–3458, Nov. 2008.

[7] A. H. Sari, M. K. Salem, and A. Shoorche, "Effect of Nitrogen Ion Implantation in Copper," *J. Fusion Energy*, vol. 30, no. 4, pp. 323–327, Aug. 2011.

[8] Cui Fuzhai and A M Vredenberg and R de Reus and F W Saris, "Formation of Nitride Cu 3 N by MeV N-Ion Implantation into Cu," *Chin. Phys. Lett.*, vol. 8, no. 10, p. 525, 1991.

[9] B. Predel (1994), O. Madelung (ed.) SpringerMaterials, Cu-N (Copper-Nitrogen) Landolt-Börnstein - Group IV Physical Chemistry 5D (Cr-Cs – Cu-Zr), https://materials.springer.com/lb/docs/sm_lbs_978-3-540-47417-3_1091, 10.1007/10086090_1091 (Springer-Verlag Berlin Heidelberg © 1994)

[10] P. Laffitte and P. Grandadam, "Sur la nitruration de quelques métaux," *Comptes Rendus Hebd. Séances Académie Sci.*, p. 1039, 1935.

[11] R. Juza and H. Hahn, "Über die Kristallstrukturen von Cu3N, GaN und InN Metallamide und Metallnitride," *Z. Für Anorg. Allg. Chem.*, vol. 239, no. 3, pp. 282–287, Oct. 1938.

[12] A. Schroelter, "Ueber das Verhalten der Metalle und einiger Verbindungen derselben zum Ammoniak bei höherer Temperatur," *Justus Liebigs Ann. Chem.*, vol. 37, no. 2, pp. 129– 152, Jan. 1841.

[13] A. Jiang, M. Qi, and J. Xiao, "Preparation, structure, properties, and application of copper nitride (Cu3N) thin films: A review," *J. Mater. Sci. Technol.*, vol. 34, no. 9, pp. 1467–1473, Sep. 2018.

[14] Z. Liu, W. Wang, T. Wang, S. Chao, and S. Zheng, "Thermal stability of copper nitride films prepared by rf magnetron sputtering," *Thin Solid Films*, vol. 325, no. 1, pp. 55–59, Jul. 1998.

[15] M. D. Reichert, M. A. White, M. J. Thompson, G. J. Miller, and J. Vela, "Preparation and Instability of Nanocrystalline Cuprous Nitride," *Inorg. Chem.*, vol. 54, no. 13, pp. 6356–6362, Jul. 2015.

[16] A. Jimenez-Morales, J. C. Galvan, R. Rodriguez, and J. J. De Damborenea, "Electrochemical study of the corrosion behaviour of copper surfaces modified by nitrogen ion implantation," *J. Appl. Electrochem.*, vol. 27, no. 5, pp. 550– 557, May 1997.

[17] L. Ge, N. Tian, Z. Lu, and C. You, "Influence of the surface nanocrystallization on the gas nitriding of Ti–6Al–4V alloy," *Appl. Surf. Sci.*, vol. 286, pp. 412–416, Dec. 2013.

[18] M. Bonvalet, X. Sauvage, D. Blavette, Intragranular nucleation of tetrahedral precipitates and discontinuous precipitation in Cu-5wt%Ag, Acta Materialia 164 (2019) 454-463.

[19] Ghenwa Zaher, Samuel Jouen, Ivan Lomakin, Nariman Enikeev, Xavier Sauvage, Influence of HPT processing conditions and tin in solid solution on the UFG structure and hardness of copper, Materials Today Communications (2021) 101746

[20] F. Guernalec and D. Busaedo, "Device and Method for Nitriding by ionic implantation of an aluminium alloy part" patent: WO/2005/085491, 15-Sep-2005.

[21] W. D. Nix and H. Gao, "Indentation size effects in crystalline materials: A law for strain gradient plasticity," J. Mech. Phys. Solids, vol. 46, no. 3, pp. 411–425, Mar. 1998.

[22] Y. Y. Lim and M. M. Chaudhri, "The effect of the indenter load on the nanohardness of ductile metals: An experimental study on polycrystalline work-hardened and annealed oxygen-free copper," Philos. Mag. A, vol. 79, no. 12, pp. 2979–3000, Dec. 1999.

[23] G. Z. Voyiadjis and M. Yaghoobi, "Review of Nanoindentation Size Effect: Experiments and Atomistic Simulation," Crystals, vol. 7, no. 10, 2017.

[24] E. Sidot, A. Kahn-Harari, E. Cesari, and L. Robbiola, "The lattice parameter of α- bronzes as a function of solute content: application to archaeological materials," Mater. Sci. Eng. A, vol. 393, no. 1, pp. 147–156, Feb. 2005.

[25] Kaveh Edalati et al, Nanomaterials by Severe Plastic Deformation: Review of Historical Developments and Recent Advances, Materials Research Letters (2022) vol 10, issue 4, pp 163-256.